

Kondo Effect in a Quantum Antidot

M. Kataoka, C. J. B. Ford, M. Y. Simmons,* and D. A. Ritchie

Cavendish Laboratory, Madingley Road, Cambridge CB3 0HE, United Kingdom

(November 2, 2018)

Abstract

We report Kondo-like behaviour in a quantum antidot (a submicron depleted region in a two-dimensional electron gas) in the quantum-Hall regime. When both spin branches of the lowest Landau level encircle the antidot in a magnetic field (~ 1 T), extra resonances occur between extended edge states via antidot bound states when tunnelling is Coulomb blockaded. These resonances appear only in alternating Coulomb-blockaded regions, and become suppressed when the temperature or source-drain bias is raised. Although the exact mechanism is unknown, we believe that Kondo-like correlated tunnelling arises from skyrmion-type edge reconstruction. This observation demonstrates the generality of the Kondo phenomenon.

One of the most well-studied many-body phenomena, the Kondo effect, arises when an isolated electronic spin is present in a sea of free electrons. A reason why the Kondo effect has attracted so much attention is that the same theoretical treatment can describe many different systems, such as metals containing magnetic impurities [1,2], weakly confined quantum dots [3–5], or even more exotic systems where the role of spin is replaced by another internal degree of freedom [6]. Quantum dots mimic magnetic impurities by electrostatic confinement of electrons, and the flexibility in tuning various parameters has recently enabled the study of Kondo phenomena in great detail [7–10]. Here, we report Kondo-like correlated tunnelling in a very different system, a quantum antidot [11–14], where electrons are confined magnetically (by the Lorentz force) around a submicron depleted region (antidot) in a two-dimensional electron gas (2DEG). Certain features of our results, such as the absence of spin splitting of the zero-bias anomaly, imply that the system cannot be described by the conventional Kondo models. We suggest that a skyrmion-type edge reconstruction around the antidot leads to an enhancement of correlated tunnelling between extended edge states via the antidot.

An impurity in a metal (or a quantum dot coupled to reservoirs) is magnetic if it contains an unpaired electronic spin. At low temperature, the second- and higher-order impurity scattering processes involving spin-flip of the localised state (Fig. 1A) is enhanced if the coupling between the localised and delocalised electrons are antiferromagnetic. This is the Kondo effect. As a result, in the metal, the resistivity increases as it is cooled down, the opposite of ordinary metallic behaviour. In a quantum dot, the transmission between reservoirs becomes enhanced. Such a Kondo resonance occurs when the dot has an unpaired spin (i.e. when the number of electrons N in the quantum dot is odd). N can be changed by, for example, varying the voltage on a gate nearby. The conductance curve as a function of gate voltage shows pairing of resonances at low temperature, as the Kondo effect increases the conductance of alternating Coulomb-blockaded regions and brings the two peaks close together (see the top-right diagram in Fig. 1A). This is often called odd-even behaviour.

Now, in terms of device structure, a quantum antidot (Fig. 1B) is quite different from a quantum dot. A magnetic field B applied perpendicular to the plane of the 2DEG quantises the kinetic energy of the electrons into Landau levels at $(n + 1/2)\hbar\omega_c$, where n (≥ 0) is an integer, $\hbar = h/2\pi$ (h : Planck's constant), and ω_c is the cyclotron frequency. Along the bulk 2DEG boundaries, the Landau levels rise in energy with the electrostatic potential, and extended edge states form where the Landau levels intersect the Fermi energy. Around the antidot, electrons form localised states, travelling phase-coherently in closed orbits. Due to the Aharonov-Bohm effect, each state encompasses an integer number of magnetic flux quanta $\phi_0 = h/e$. Therefore, the average area S_i enclosed by the i th state is quantised as $BS_i = i\phi_0$. The states are filled up to the Fermi energy (filled circles in Fig. 1B) and those above are empty (open circles). When B increases, each state shrinks in area (in order to keep BS_i constant), moving towards the centre of the antidot, and accumulating a net negative charge. Because the states are all quantised, the net charge cannot relax until enough charge ($-e/2$) has built up, at which point an electron leaves and the net charge jumps to $e/2$ [13]; the process then repeats with period $\Delta B = h/eS$, where S is the area enclosed by a state at the Fermi energy. This periodic depopulation can be observed in conductance measurements if the current-carrying extended edge states are brought close to the antidot so that electrons tunnel between them (see Fig. 1B). Here, the conductance decreases on resonance, because the resonance enhances backscattering (between opposite edges). This resonance process when sweeping B resembles that when sweeping gate voltage in quantum dots: off resonance, tunnelling is Coulomb blocked due to the discreteness of the electronic charge.

Samples were fabricated from a GaAs/AlGaAs quantum-well structure containing a 2DEG situated 300 nm below the surface with a sheet density $3 \times 10^{15} \text{ m}^{-2}$ and mobility $500 \text{ m}^2/\text{Vs}$. On top of the substrate, metal Schottky gates (10 nm NiCr/30 nm Au) were patterned by electron-beam lithography (top-right inset of Fig. 1B). A second metal layer (30 nm NiCr/70 nm Au) was patterned on top of 350 nm cross-linked polymethylmethacrylate (PMMA) [15] in order to contact the central dot gate so that voltages can be applied to the three gates independently. A negative voltage on the dot gate, $0.3 \mu\text{m}$ on a side, creates an antidot by depleting electrons underneath. The depleted region can be approximated to be circular, with a radius of $\sim 0.36 - 0.40 \mu\text{m}$, depending on the voltage used; the radius is deduced from the Aharonov-Bohm period ΔB . The two side gates, which are used to bring the extended edge states close to the antidot, form parallel one-dimensional constrictions, each with lithographic width $0.7 \mu\text{m}$ and length $0.3 \mu\text{m}$. The measurements were performed in a dilution refrigerator with a base temperature $\sim 25 \text{ mK}$.

The conductance measurements were performed as follows. A $5 \mu\text{V}$ AC excitation voltage at 77 Hz was applied between the ohmic contacts 1 and 3 shown in the bottom-left inset to Fig. 2 and the current I was measured using a lock-in amplifier. Simultaneously, the diagonal voltage drop V_{dg} between the contacts 2 and 4 was measured, and the antidot conductance was calculated as $G_{\text{ad}} = I/V_{\text{dg}}$. In the quantum Hall regime (with the correct direction of edge current flow), this four-terminal measurement gives the 'true' [16] two-terminal conductance $G_{\text{ad}} = \nu_c e^2/h$, where ν_c is the number of filled Landau levels in the antidot constrictions [17]. The filling factors in the constrictions and the coupling between the extended edge states and the antidot states can be tuned by the voltages on the side gates, and they were kept as symmetric as possible throughout the measurements.

The number of Landau levels forming bound states around the antidot is defined by the number of edge states transmitted through the constrictions. Figure 2 shows a typical G_{ad} vs B curve taken at 25 mK when the two spins of the lowest Landau level encircle the antidot; ν_c decreases from 2 to 1 as B increases. At low B where G_{ad} is close to the $\nu_c = 2$ quantum-Hall plateau value $2e^2/h$, a series of pairs of dips (two dips per ΔB) can be seen. As B increases, and as the coupling between the leads and the antidot becomes stronger (because the edge states move towards the centre of the constrictions), the amplitude of the dips increases. Also, the gaps inside pairs (intra-pair gaps) seem to be filled up, and eventually the pairs become unrecognisable as two independent dips above 1.3 T as G_{ad} approaches the $\nu_c = 1$ plateau value e^2/h . Very similar conductance curves have been observed between the $\nu_c = 2$ and 1 plateaux with different gate-voltage settings and with different B ranging from 0.8 to 1.5 T in many samples and on many thermal cycles. At higher magnetic fields (> 3 T), the pairing of the resonances disappears, but instead the oscillations become pure double-frequency [11, 14].

These pairs may simply seem to be spin-split pairs (each dip corresponding to a resonance of either spin). The difference in the amplitude of alternating dips may be an indication of different coupling strength for each spin. However, curve fitting (top-right diagram in Fig. 2) shows that the feature in the intra-pair gap cannot be explained by such a simplistic model [18]. Strikingly, the paired resonances in Fig. 2, if shown upside down, look very similar to Coulomb-blockade oscillations with Kondo resonances in quantum dots (top-right diagram in Fig. 1A). We argue that the discrepancy in the intra-pair gaps is caused by Kondo resonances, based on the results from the nonequilibrium and temperature activation measurements described below.

The behaviour of Kondo resonances under nonequilibrium conditions has been well studied in quantum dots [7–10]. Under a finite source-drain bias, mismatch in the chemical potentials of the source and drain suppresses the Kondo resonance. In our experiments, when a small source-drain DC bias V_{sd} is applied in addition to the AC excitation, the ‘Kondo feature’ filling each intra-pair gap vanishes, leaving two well-defined dips as shown in Fig. 3A. The Kondo features appear as horizontal red/dark lines (zero-bias anomaly) around $V_{\text{sd}} = 0$ when G_{ad} is plotted in colour-scale against V_{sd} and B (Fig. 3B). Note that here the horizontal axis is B instead of V_g , as is normally the case for quantum dots. The zero-bias anomaly becomes stronger as B , and hence the coupling, increase. The diamond-shaped structures of red lines arise because each resonance splits into two under a finite bias due to the difference in the chemical potentials of the two leads. From the height of each diamond, the energy to add an extra electron (charging energy) can be estimated to be $\sim 60 \mu\text{eV}$. When the coupling is made even stronger, the zero-bias anomaly is still clearly visible, whereas the diamond structures are smeared out due to weak confinement (Fig. 3C).

Increasing temperature T suppresses our Kondo feature, leaving the intra-pair gaps better defined (Fig. 3D and E). At around 190 mK, the intra-pair and inter-pair gaps become almost indistinguishable. At lower B where intra-pair gaps are almost as well defined as inter-pair gaps, increasing T broadens each dip, and the conductance in both gaps decreases (as expected without the Kondo effect). However, at higher B , the conductance in the intra-pair gaps *increases*. Because the feature disappears into the noise level at relatively low T , it was not possible to study the temperature dependence in more detail, e.g. to determine the Kondo temperature T_K , which normally marks the crossover between logarithmic (high

T) and power-law (low T) behaviours. We note that the amplitude of our Kondo feature decreases monotonically as T increases.

The above behaviour of the antidot conductance is qualitatively very similar to that of Kondo resonances in a quantum dot. It appears that as the antidot states are depopulated one by one when B is increased, a localised magnetic moment arises when there is an unpaired electronic spin. Then, when the coupling between the extended and antidot edge states is strong, Kondo resonances enhance the tunnelling through the antidot in the Coulomb-blockaded region. Stronger coupling results in larger T_K , and hence the zero-bias anomaly is more pronounced in the region closer to the $\nu_c = 1$ plateau (where the wavefunctions of the extended and antidot states strongly overlap).

However, there is a crucial difference in our results from those in quantum dots. In a quantum dot in a comparable magnetic field, the Zeeman energy $E_Z = |g|\mu_B B$ (μ_B is Bohr magneton and $g = -0.44$ in bulk GaAs) usually splits the zero-bias anomaly into two parallel lines separated by $2E_Z/e$. The Kondo resonance is suppressed at $V_{sd} = 0$ because spin degeneracy is lifted [7,8,10]. At $B = 1.2 T$, $E_Z = 30 \mu\text{eV}$, but the width of our zero-bias anomaly is $\sim 20 \mu\text{V}$. Thus, the energy gap between the opposite spin states must be at most $10 \mu\text{eV}$, and probably much smaller. This is at least a factor of 3 less than E_Z .

One possible explanation for this lack of spin-splitting is to consider an accidental degeneracy between neighbouring orbital states with opposite spins. This might occur if E_Z happened to be close to an integer multiple of the single-particle energy spacing ΔE_{sp} (the difference in potential energy between neighbouring states; see Fig. 1C). However, since $\Delta E_{\text{sp}} \propto 1/B$ if a constant potential is assumed, the ratio $E_Z/\Delta E_{\text{sp}} \propto B^2$ would not stay constant over a wide range of B . As we have observed the effect under many different conditions, it is highly unlikely that this accidental degeneracy is the cause.

Another important issue in our experiments is that the conductance dips saturate at e^2/h (Fig. 2), forming the $\nu_c = 1$ plateau as B increases and the oscillations die away. The existence of the $\nu_c = 1$ plateau implies that the extended edge states of the lower spin state are perfectly transmitted through the constrictions, and not coupled to the antidot. This causes another difficulty in the interpretation, because, for ordinary Kondo resonances to occur, both spins in the leads need to be coupled to the localised state.

It is likely that the edge-state picture shown so far needs to be modified to a many-body picture. Recently, we have demonstrated that a self-consistent treatment of the antidot potential is important, especially at higher B [14]. Taking into account the formation of two concentric compressible rings (where states are partially filled, and are pinned at the Fermi energy; see Fig. 1D) [19], we have successfully explained double-frequency Aharonov-Bohm oscillations observed at higher B [11]. However, this is not yet enough for the Kondo effect, as either only one spin (outer ring) would be coupled to the leads, or, if both spins were coupled to the leads, there would be no $\nu_c = 1$ plateau.

It has been shown that in a relatively weak magnetic field, an excited state of a $\nu = 1$ quantum Hall liquid is not simply a spin flip, but rather, a complicated spin texture, called a skyrmion [20], which forms due to strong correlations. Recent work has shown that skyrmion-type edge reconstruction is important in quantum dots in the quantum Hall regime [21,22]. If we assume that such correlated states form in the regions of the antidot and extended edge states where the local filling factor is $1 < \nu < 2$ (Fig. 1E), electrons with both spins there would be allowed to tunnel, whether the $\nu \leq 1$ edge states are coupled or not. The excitation

energy of correlated states is typically smaller than E_Z . If two configurations, in which the total spin differs by one, are (almost) degenerate, this may allow spin-flip tunnelling. It is uncertain, however, whether the odd-even behaviour can occur with such strongly correlated states.

In summary, we have shown that an antidot in the quantum Hall regime qualitatively exhibits all the features of the Kondo effect, despite the lack of an obvious reason for spin degeneracy. We have suggested possible ways in which the edge-state picture may be modified to take account of interactions. The fact that the antidot is an open system further complicates the problem, in comparison with quantum dots, where only a limited number of states are considered. A detailed theoretical calculation is needed to determine the edge-state structure that gives rise to the Kondo-like behaviour in an antidot.

This work was funded by the UK EPSRC. We thank I. Smolyarenko, N. R. Cooper, B. D. Simons, A. S. Sachrajda, H.-S. Sim and V. Falco for useful discussions.

References and Notes

- [1] J. Kondo, Prog. Theor. Phys. **32**, 37 (1964).
- [2] For a review, see A. C. Hewson, *The Kondo Problem to Heavy Fermions* (Cambridge University Press, Cambridge, 1993).
- [3] L. I. Glazman and M. E. Raikh, JETP Lett. **47**, 452 (1988).
- [4] T. K. Ng and P. A. Lee, Phys. Rev. Lett. **61**, 1768 (1988).
- [5] Y. Meir, N. S. Wingreen, and P. A. Lee, Phys. Rev. Lett. **70**, 2601 (1993).
- [6] D. L. Cox and A. Zawadowski, Advances in Physics **47**, 599 (1998).
- [7] D. Goldhaber-Gordon, H. Shtrikman, D. Mahalu, D. Abusch-Magder, U. Meirav, and M. A. Kastner, Nature **391**, 156 (1998).
- [8] S. M. Cronenwett, T. H. Oosterkamp, and L. P. Kouwenhoven, Science **281**, 540 (1998).
- [9] W. G. van der Wiel, S. De Franceschi, T. Fujisawa, J. M. Elzerman, S. Tarucha, and L. P. Kouwenhoven, Science **289**, 2105 (2000).
- [10] M. Keller, U. Wilhelm, J. Schmid, J. Weis, K. von Klitzing, and K. Eberl, Phys. Rev. B **64**, 033302 (2001).
- [11] C. J. B. Ford, P. J. Simpson, I. Zailer, D. R. Mace, M. Yosefin, M. Pepper, D. A. Ritchie, J. E. F. Frost, M. P. Grimshaw, and G. A. C. Jones, Phys. Rev. B **49**, 17456 (1994).
- [12] V. J. Goldman and B. Su, Science **267**, 1010 (1995).
- [13] M. Kataoka, C. J. B. Ford, G. Faini, D. Mailly, M. Y. Simmons, D. R. Mace, C.-T. Liang, and D. A. Ritchie, Phys. Rev. Lett. **83**, 160 (1999).
- [14] M. Kataoka, C. J. B. Ford, G. Faini, D. Mailly, M. Y. Simmons, and D. A. Ritchie, Phys. Rev. B **62**, R4817 (2000).
- [15] I. Zailer, J. E. F. Frost, V. Chabasseur-Molyneux, C. J. B. Ford, and M. Pepper, Semicond. Sci. Technol. **11**, 1235 (1996).
- [16] ‘True’ in the sense that the two-terminal conductance is not affected by the series resistance of the experimental circuit.
- [17] M. Büttiker, Phys. Rev. Lett. **57**, 1761 (1986).

- [18] In Ref. 14, we gave a model with transmission and reflection resonances in an attempt to explain similar oscillations, however this model does not explain the temperature and source-drain bias measurements shown here.
- [19] D. B. Chklovskii, B. I. Shklovskii, and L. I. Glazman, Phys. Rev. B **46**, 4026 (1992).
- [20] S. L. Sondhi, A. Karlhede, S. A. Kivelson, and E. H. Rezayi, Phys. Rev. B **47**, 16419 (1993).
- [21] P. Hawrylak, C. Gould, A. Sachrajda, Y. Feng, Z. Wasilewski, Phys. Rev. B **59**, 2801 (1999).
- [22] C. Tejedor and L. Martin-Moreno, Phys. Rev. B **63**, 35319 (2001).

* Present address: School of Physics, University of New South Wales, Sydney 2052, Australia.

Figures

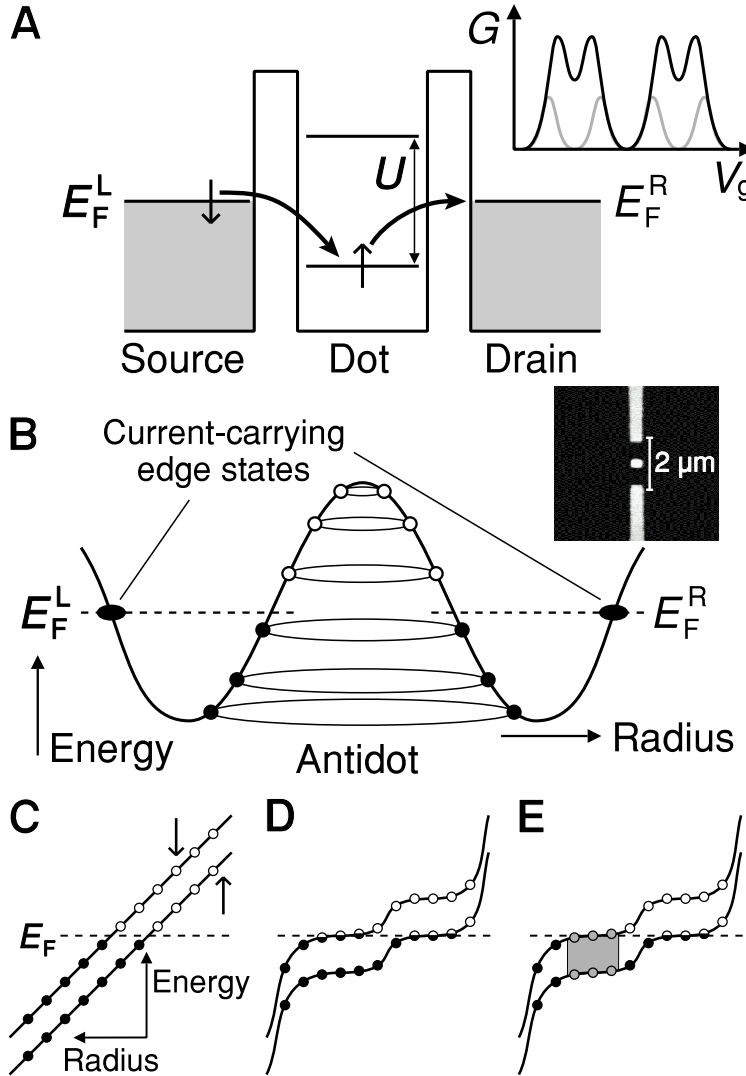


FIG. 1. (A) Spin-flip tunnelling through a Coulomb-blockaded quantum dot (U : charging energy). The Kondo effect enhances higher-order processes of such tunnelling at low temperature. The top-right diagram shows the conductance G of the dot versus gate voltage V_g with (black) and without (grey) Kondo resonances. (B) A Landau level near the antidot and constrictions. The circular orbits of filled and empty states are represented by filled and open circles, respectively. Filled ovals represent the extended edge states, which determine the current through the sample. Top-right inset: a scanning electron micrograph of a device prior to the second-layer metallisation. (C) A Landau level near the Fermi energy around the antidot with an accidental spin degeneracy between neighbouring states. (D) Self-consistent potential with two compressible regions (one for each spin). (E) As D but with correlated states (shaded in grey) in the $1 < \nu < 2$ region.

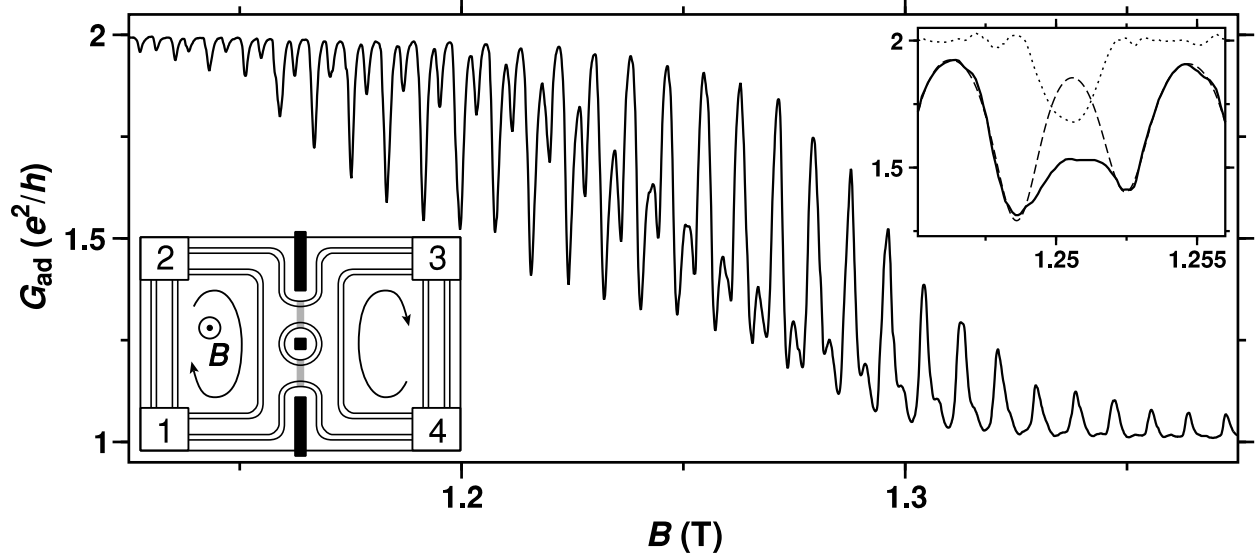


FIG. 2. A typical antidot conductance G_{ad} vs B curve at 25 mK between the $\nu_c = 2$ and 1 plateaux. The pairs of dips imply backscattering resonances through alternating spin states. However, detailed study of the oscillations indicates that Kondo resonances occur inside the pairs. Top-right inset: the results of a fit conducted for the pair around $B = 1.25$ T by using four dips proportional to the derivative of Fermi function. The solid line is the experimental curve and the dashed line is the fit. The fit was performed in such a way that the curves between the pairs match as well as possible (but two dips for the pair can never fit the curve inside the pair). The dotted line is the difference between the experimental curve and the fit (offset by $2e^2/h$). Bottom-left inset: schematic showing the sample geometry with four edge states (solid lines), two of each spin. Arrows indicate the direction of electron flow. Grey lines show where tunnelling occurs between the extended edge states and the antidot states. The numbered rectangles on the corners represent ohmic contacts.

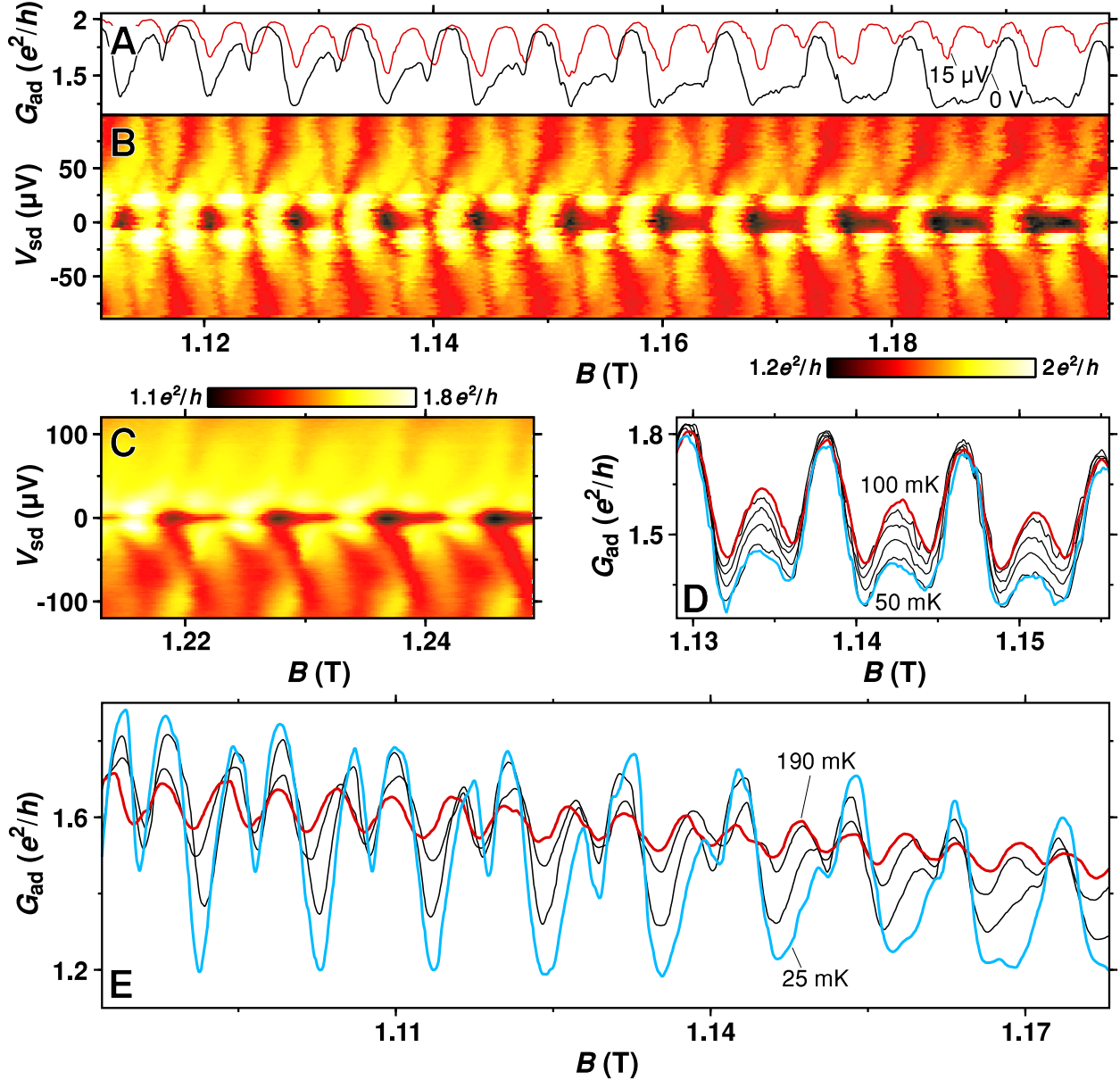


FIG. 3. (A) G_{ad} vs B curves at 25 mK with source-drain bias $V_{\text{sd}} = 0$ V (black curve) and with $V_{\text{sd}} = 15$ μV (red curve). The odd-even feature seen at zero bias almost disappears when a small bias is applied. (B) Colour-scale plot of the differential conductance G_{ad} against B and V_{sd} . As the coupling between the leads and antidot becomes stronger (as B increases), the zero-bias anomaly becomes stronger. (C) DC-bias measurements plotted in the same manner as in B. Here, the coupling is larger, so the diamond structure is unclear, whereas the zero-bias anomaly is clearly visible. (D) Temperature dependence of G_{ad} vs B with small increments of temperature (~ 10 mK). The feature filling the gap inside each pair weakens as the temperature T is increased, leaving the gaps inside pairs *better* defined at *higher* temperature, which is a signature of the Kondo effect. (E) Temperature dependence of G_{ad} vs B over a wide range of T . The odd-even feature at low T (blue curve) disappears as T is raised to 190 mK (red curve), showing almost double-frequency oscillations.